



## An indirect boundary-element method for slow viscous flow in a bounded region containing air bubbles

A. R. M. PRIMO<sup>1,3</sup>, L. C. WROBEL<sup>1</sup> and H. POWER<sup>2</sup>

<sup>1</sup>*Brunel University, Department of Mechanical Engineering, Uxbridge, Middlesex UB8 3PH, U.K.*

<sup>2</sup>*Wessex Institute of Technology, Ashurst Lodge, Ashurst, Southampton SO40 7AA, U.K.*

<sup>3</sup>*On leave from Department of Mechanical Engineering, Universidade Federal de Pernambuco, Recife, Brazil*

Received: 18 December 1997; accepted in revised form 12 April 1999

**Abstract.** This paper presents a novel formulation of the completed indirect boundary-element method to study the shrinkage of air bubbles on a slow viscous flow in a bounded region subject to surface tension. The formulation has application to viscous sintering, a process for manufacturing high-quality glass by means of sol-gel processing. The theoretical background is explained in detail, including mathematical proofs of existence and uniqueness of solutions. Numerical results are included and compared to analytical and previous numerical solutions.

**Key words:** boundary-element method, viscous sintering, Stokes flow, surface tension.

### 1. Introduction

Sintering is a process in which a granular compact of metals, ionic crystals or glasses consisting of many particles, is heated to such a temperature that the mobility of the material is sufficient to make contiguous particles coalesce. In the production of aerogels and glassy materials, the material transport can be modelled as a viscous incompressible Newtonian flow, driven solely by surface tension, and the process is known as viscous sintering.

A good theoretical understanding of the densification kinetics is needed to produce dense and homogeneous compacts. Because of the complexity of the phenomenon, scientists studying sintering have long been interested in the behaviour of simple systems which are representative of contacting particles. More recently, numerical techniques have been developed for viscous sintering problems. The present work focusses on a new boundary-integral formulation for the problem and its solution using the boundary-element method.

The boundary element method (BEM) was initially applied by Kuiken [1–2] and van de Vorst *et al.* [3–4] to describe the sintering of simple two-dimensional and axisymmetric systems. Kuiken [1] defined the problem in terms of the stream-function-vorticity formulation and found the solution using a system of two coupled integral equations, for harmonic and bi-harmonic functions. However, numerical problems occurred due to inaccuracies in computing the derivative of the curvature, which was required in that particular formulation. Van de Vorst *et al.* [3–4] defined the problem in terms of the primitive variables and found the solution using a Lorentz's [5] direct integral representation formulae for the Stokes flow, given by the sum of a single- and a double-layer potentials whose densities are the surface traction and velocity, respectively. By prescribing the surface traction, they obtained a Fredholm integral equation of the second kind for the unknown surface velocity which is free from the problem of computing the tangential derivative of the curvature. This formulation allowed the extension of

Kuiken's range of solutions. However, by directly applying Lorentz's representation formulae to the present second-kind boundary-value problem, an integral equation is found which is not uniquely solvable. This requires the completion of the integral operator in order to remove the corresponding eigenvalues through a mathematical manipulation of the integral equation without changing the physical meaning of the solution.

In the case of a simply-connected domain, *e.g.* the deformation of an arbitrarily-shaped single viscous drop, van de Vorst *et al.* [3] completed the operator by adding a suitable linear combination of rigid body motions, which by definition do not alter the original boundary conditions. For the case of a multiply-connected domain, *e.g.* the sintering of a viscous drop with internal air bubbles, besides the rigid body terms, it was necessary to add a single- and a double-layer potential at each internal bubble to remove the eigenvalues associated with the internal surfaces. The kernels of these layer potentials are given by the velocity and surface traction of the flow field due to point sinks located at the interior of each bubble, coupled with zero pressure; their densities are the same as those of Lorentz's potentials, *i.e.* the surface traction and velocity at the bubble surfaces.

Power and Miranda [6] explained how integral equations of the second kind can be obtained for general three-dimensional Stokes flows around a single particle using an indirect integral-equation formulation in terms of a double-layer potential. They observed that, although the double-layer potential can only represent those flow fields corresponding to surfaces which are force- and torque-free, the representation should be completed by adding terms that give arbitrary total force and torque in suitable linear combinations. The extension of Power and Miranda's method to multiple particles in an unbounded flow was given by Power [7] and Karrila *et al.* [8], and to a particle in a bounded flow by Power and Miranda [9] and Karrila and Kim [10]. In the latter case, the flow appears as external when looking from the particle, but as internal when looking from the exterior contour. The second-kind formulation for this problem is not a trivial extension, since the completeness procedure of the deficient range of the double-layer potential requires special care due to the existence of an exterior container. Applications to two-dimensional problems have been reported by Power [11–13], where particular attention was paid to the Stokes' paradox.

Karrila *et al.* [8] and Karrila and Kim [10] gave an elegant mathematical interpretation of the above method, by observing its relation to Wielandt's deflation. By removing the end points of the spectrum of the integral operator of an integral equation of the second kind, arising from a double-layer representation without completion, they moved those eigenvalues without affecting the rest of the eigenvalues, thus providing a bounded invertible operator and then allowing for iterative solutions. Karrila and Kim [10] called Power and Miranda's [6] approach the *Completed Double-Layer Boundary-Integral-Equation Method* (CDL-BIEM), since it involves the idea of completing the deficient range of the double-layer operator; the CDL-BIEM technique, however, has sometimes been attributed to Karrila and Kim. It is important to recognize here that Power and Miranda's completed method is an extension, to the Stokes equations, of Mikhlin's results [14] for the exterior Dirichlet problem for Laplace's equation. More details on the completed approach can be found in the books of Kim and Karrila [15], Pozrikidis [16] and Power and Wrobel [17].

The main objective of the present work is to propose an indirect integral-equation formulation for two-dimensional viscous sintering in terms of only one surface potential. The approach presented here is an extension of Power and Miranda's [6] technique to the present second-kind boundary-value problem. The potential problems with the Stokes paradox are addressed when discussing the uniqueness of solutions. The method is constructive and re-

quires a simpler computer implementation than previous methods, particularly in the case of multiply-connected domains.

## 2. Mathematical formulation

The problem will be defined here in terms of primitive variables, similar to van der Vorst *et al.* [3–4]. Firstly, the simply-connected domain case will be considered, for which the problem is defined by the Stokes creeping flow equations

$$\mu \frac{\partial^2 u_i}{\partial x_j \partial x_j} - \frac{\partial p}{\partial x_i} = 0, \quad (1)$$

$$\frac{\partial u_i}{\partial x_i} = 0 \quad (2)$$

for any point  $x \in \Omega(t)$ . Here,  $\Omega$  is the bounded domain interior to the drop surface  $S$ , assumed to be of the Lyapunov type,  $\mathbf{u}$  is the velocity vector,  $p$  is the pressure and  $\mu$  the dynamic viscosity.

The interior flow field has to satisfy the following boundary condition

$$\sigma_{ij} n_j = \gamma \kappa n_i \quad \text{on } S(t), \quad (3)$$

where

$$\sigma_{ij} = -p \delta_{ij} + \mu \left( \frac{\partial u_i}{\partial x_j} + \frac{\partial u_j}{\partial x_i} \right) \quad (4)$$

is the stress tensor,  $\sigma_{ij} n_j$  is the surface traction,  $\gamma$  is the surface tension,  $\kappa$  is the surface curvature, and  $\mathbf{n}$  is the unit normal vector outward to the drop. Equation (3) represents a balance of surface tension and fluid traction forces on the exterior boundary.

The rate of deformation is determined by the kinematic boundary condition at  $S$ , which states that the normal component of the fluid velocity at a point  $\xi$  of the drop's surface is equal to the normal component of the surface velocity at that point

$$\frac{dx_i}{dt} n_i = u_i n_i \quad \text{at } \xi \in S(t). \quad (5)$$

If the quasi-static character of the motion is taken into account, the boundary-value problem (1–3) may be solved for a given drop shape  $S(t)$ . With the computed surface velocity  $u_i(\xi, t)$  and a time step  $\Delta t$ , the shape of the deformed drop  $S(t + \Delta t)$  can be determined by use of the kinematic condition (5). The scheme starts with a given initial drop shape  $S(t = 0)$ ; then, at each instant in time, Equations (1–3) define a second-kind boundary-value problem for the Stokes equations.

At each instant in time the force and torque yielded by the surface tension upon the drop surface  $S(t)$  have to be zero, *i.e.*

$$\int_{S(t)} \sigma_{ij}(\mathbf{u}, p) n_j \phi_i^l dS = \int_{S(t)} \gamma \kappa n_i \phi_i^l dS = 0, \quad (6)$$

where  $\varphi^l, l = 1, 2, 3$ , are the three linearly-independent rigid body vectors, taken as:

$$\varphi_i^l = \delta_{il} \quad \text{for } l = 1, 2 \quad \text{and} \quad \varphi^3(x) = (x_2, -x_1). \tag{7}$$

Equation (6) follows from Lorentz’s reciprocal Theorem [5], given that a regular Stokes flow field  $(\mathbf{u}, p)$  is sought at the domain interior to the surface  $S(t)$ , and that any rigid body fluid motion with zero associated pressure is also a regular interior Stokes flow field with zero stress. The solvability condition (6) can also be derived by a direct application of the Gauss theorem to Equation (1).

Instead of using a direct BEM formulation, as in van de Vorst *et al.* [3–4], we will seek the solution of the present second-kind boundary-value problem in terms of a single-layer potential alone, with unknown vector density  $\Phi$  [16, p. 143],

$$u_i(x) = - \int_S u_i^j(x, y) \Phi_j(y) dS_y \tag{8}$$

for every  $x \in \Omega$ , where

$$u_i^j(x, y) = - \frac{1}{4\pi\mu} \left( \delta_{ij} \log \left( \frac{1}{r} \right) + \frac{(x_i - y_i)(x_j - y_j)}{r^2} \right), \quad r = |x - y| \tag{9}$$

is the two-dimensional fundamental solution of the Stokes equations, also known as the stokeslet [18], applied at point  $y$  and oriented in the  $j$ th direction. The pressure field is given as a distribution of the pressure corresponding to the single-layer potential, *i.e.*

$$p(x) = - \frac{1}{2\pi} \int_S \frac{\partial}{\partial x_j} \left( \log \frac{1}{r} \right) \Phi_j(y) dS_y. \tag{10}$$

Applying the boundary condition (3) to the flow field described by (8) and (10), and using the discontinuity property of the surface forces of a single-layer potential across the density-carrying surface  $S$ , we obtain the following linear Fredholm integral equation of the second kind for the unknown density  $\Phi$ :

$$\frac{1}{2} \Phi_i(\xi) - \int_S K_{ji}(y, \xi) \Phi_j(y) dS_y = \gamma \kappa(\xi) n_i(\xi) \tag{11}$$

for every  $\xi \in S$ , where the kernel

$$\begin{aligned} K_{ji}(y, \xi) &= - \frac{1}{\pi} \frac{(y_i - \xi_i)(y_j - \xi_j)(y_k - \xi_k)}{r^4} n_k(\xi) \\ &= \frac{1}{\pi} \frac{\partial r}{\partial \xi_i} \frac{\partial r}{\partial \xi_j} \frac{\partial \log r}{\partial n_\xi} = \frac{1}{\pi} \frac{\partial r}{\partial \xi_i} \frac{\partial r}{\partial \xi_j} \left( \frac{\cos(\mathbf{n}(\xi), \mathbf{r})}{r} \right) \end{aligned}$$

is discontinuous but not singular since  $\cos(\mathbf{n}(\xi), \mathbf{r})/r \rightarrow \kappa(\xi)/2$  as  $y \rightarrow \xi$  [19, p. 299].

The adjoint to the homogeneous form of Equation (11), given by

$$\frac{1}{2} \varphi_i^l(\xi) - \int_S K_{ij}(\xi, y) \varphi_j^l(y) dS_y = 0 \tag{12}$$

has three linearly-independent eigensolutions corresponding to the rigid body motions given by Equation (7). Therefore, the homogeneous form of Equation (11) also has three linearly-independent eigensolutions,  $\Psi^l, l = 1, 2, 3$ , that are generally unknown. According to Fredholm's alternative, Equation (11) has a solution if and only if the inhomogeneous term is orthogonal to the rigid body vectors, *i.e.*

$$\int_S \gamma \kappa n_i \varphi_i^l dS = 0, \quad l = 1, 2, 3.$$

This will always be the case, according to the solvability condition given by Equation (6). Nevertheless, the solution of Equation (11) is nonunique, since we can add to it any linear combination of the eigensolutions  $\Psi^l, l = 1, 2, 3$ .

To remove the above eigenfunctions, it is necessary to add to the original Equation (11) a term that is linearly proportional to the rigid body vector  $\varphi^l, l = 1, 2, 3, i.e.$

$$\frac{1}{2} \Phi_i(\xi) - \int_S K_{ji}(y, \xi) \Phi_j(y) dS_y + \varphi_i^l(\xi) \beta_l = \gamma \kappa(\xi) n_i(\xi). \tag{13}$$

It is convenient, for later use, to choose  $\beta$  as:

$$\beta_l = \int_S \Phi_i \varphi_i^l dS \quad l = 1, 2, 3. \tag{14}$$

The addition of this new term to Equation (11) does not alter the nature of the problem since for any admissible inhomogeneous term, *i.e.* when the solvability condition (6) is satisfied, the vector  $\beta$  will end up being zero.

In order to prove the above statement, the new integral Equation (13) is initially multiplied by the rigid body vector,  $\varphi^n$ , at a point on the surface  $S(\xi)$ , and the resulting expression integrated with respect to  $\xi$ . Making use of the solvability condition (6) and Equation (12) we obtain the result

$$\frac{1}{2} \int_S \Phi_i(\xi) \varphi_i^n(\xi) dS_\xi - \int_S \Phi_j(y) [\frac{1}{2} \varphi_j^n(y)] dS_y + \beta_l \int_S \varphi_i^n(\xi) \varphi_i^l(\xi) dS_\xi = 0 \tag{15}$$

or

$$\beta_l \int_S \varphi_i^n(\xi) \varphi_i^l(\xi) dS_\xi = 0. \tag{16}$$

The above linear algebraic system for  $\beta_1, \beta_2, \beta_3$  only admits the trivial solution, because the determinant of Equation (16) has the term

$$\int_S \varphi_i^n \varphi_i^l dS, \quad n, l = 1, 2, 3$$

as element in its  $l$ th row and  $n$ th column, and is thus the Gram determinant for the vector functions  $\varphi^1, \varphi^2$  and  $\varphi^3$  with a nonvanishing value, on account of the linear independence of  $\varphi^k, k = 1, 2, 3$  [19, p. 62].

Although the original integral Equation (11) and the completed Equation (13) are identical for any admissible surface forces, the former does not have a unique solution whilst the latter

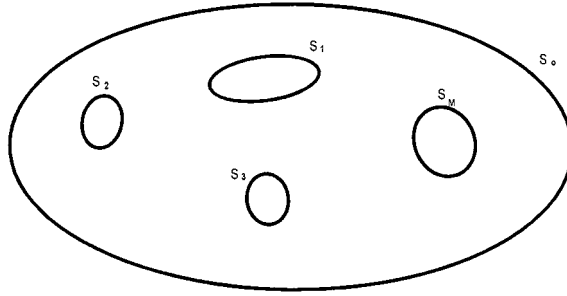


Figure 1. Viscous region with surface  $S_0$  containing air bubbles.

does. A proof is given in Appendix A, based on the fact that the homogeneous equation corresponding to (13) only admits a trivial solution.

### 2.1. VISCOUS DROP WITH INTERNAL BUBBLES

Consider now several compressible gas bubbles inside a viscous drop, as shown in Figure 1. Let  $\Omega$  be the fluid domain exterior to the bubbles and interior to the drop surface  $S_0$ . The fluid region consists of a multiply-connected domain bounded externally by  $S_0$  and internally by the surfaces  $S_1 \dots S_M$ . The symbol  $S$  denotes the total surface, *i.e.*  $S = S_0 \cup S_1 \cup \dots \cup S_M$ .

The flow field  $(\mathbf{u}, p)$  satisfies Equations (1) and (2) for all  $x$  belonging to  $\Omega$ , and the following boundary conditions

$$\sigma_{ij}(\mathbf{u}(\xi), p(\xi))n_j(\xi) = \pm\gamma\kappa(\xi)n_i(\xi) - p^l n_i(\xi) \quad \text{for every } \xi \in S_l \quad (17)$$

with  $l = 0, 1, 2, \dots, M$ , where the  $+$  sign corresponds to the exterior surface  $S_0$  and the  $-$  sign to each of the internal surfaces  $S_1, S_2, \dots, S_M$ . The normal vector  $\mathbf{n}$  is exterior to the flow domain at the surface  $S_0$ , but interior to  $\Omega$  at the surfaces  $S_1, S_2, \dots, S_M$ .

The pressure  $p^0$  at the external boundary is zero, but the pressure  $p^l, l = 1, 2, \dots, M$  at the internal gas bubbles will increase as their volume decrease. In the numerical examples, however, all bubble pressures are assumed to be zero in order that results for the present formulation can be compared with analytical and numerical solutions available in the literature.

The flow field is also subject to the solvability condition

$$\int_{S_0(t)} \sigma_{ij}(\mathbf{u}, p)n_j\varphi_i^l dS = \int_{S(t)-S_0(t)} \sigma_{ij}(\mathbf{u}, p)n_j\varphi_i^l dS, \quad l = 1, 2, 3. \quad (18)$$

As before, if the flow field is solely represented in terms of a single-layer potential with a density-carrying surface  $S$ , the resulting system of linear Fredholm integral equations of the second kind obtained by imposing the surface traction boundary conditions (17) does not have a unique solution. This is because its corresponding homogeneous system

$$\frac{1}{2}\Phi_i^o(\xi) - \int_{S_0} K_{ji}(y, \xi)\Phi_j^o(y) dS_y - \int_{S-S_0} K_{ji}(y, \xi)\Phi_j^o(y) dS_y = 0 \quad (19)$$

for every  $\xi \in S_0$ , and

$$-\frac{1}{2}\Phi_i^o(\xi) - \int_{S_j} K_{ji}(y, \xi)\Phi_j^o(y) dS_y - \int_{S-S_j} K_{ji}(y, \xi)\Phi_j^o(y) dS_y = 0 \quad (20)$$

for every  $\xi \in S_j, j = 1, 2, \dots, M$ , has  $M + 3$  linearly independent eigensolutions.

A single-layer potential with density given by any nontrivial solution of the above system will represent three linearly independent flow fields in  $\Omega$ , *i.e.*

$$\begin{aligned} \mathbf{u}(x) &= \boldsymbol{\varphi}^l(x) \quad \text{for every } x \in \Omega, \quad l = 1, 2, 3 \\ p(x) &= 0 \end{aligned} \tag{21}$$

according to the zero surface traction conditions in (19) and (20). Now, by the continuity property of the velocity field of a single-layer potential across its density-carrying surface, and the uniqueness of solution of first-kind boundary-value problems for the Stokes equations, it follows that such single-layer potential also represents three linearly independent flow fields in the domain  $\Omega_j, j = 1, 2, \dots, M$ , interior to any of the surfaces  $S_j$ , given by:

$$\begin{aligned} \mathbf{u}(x) &= \boldsymbol{\varphi}^l(x) \quad x \in \Omega_j, \quad l = 1, 2, 3, \\ p(x) &= C(\text{constant}). \end{aligned} \tag{22}$$

Taking the limit of the surface traction of the single-layer potential at any of the surfaces  $S_j, j = 1, 2, \dots, M$ , coming from the domain  $\Omega_j$ , and using the corresponding interior flow field (22), we have:

$$\frac{1}{2}\Phi_i^o(\xi) - \int_{S_j} K_{ji}(y, \xi)\Phi_j^o(y) dS_y - \int_{S-S_j} K_{ji}(y, \xi)\Phi_j^o(y) dS_y = Cn_i(\xi) \tag{23}$$

for every  $\xi \in S_j$ .

Subtracting Equation (20) from (23), we observe that the system (19) and (20) possesses the following eigensolutions at each of the internal surfaces  $S_j, j = 1, 2, \dots, M$ :

$$\Phi_i^o(\xi) = Cn_i(\xi) \quad \text{for every } \xi \in S_j. \tag{24}$$

Substituting the above eigensolutions in Equation (19), *i.e.* in each of the integrals with surface  $S_j$  for  $j = 1, 2, \dots, M$ , and using the property that every single-layer potential with the normal vector as a surface density yields zero velocity and traction at any point exterior to its density-carrying surface, we see that Equation (19) reduces to the adjoint of Equation (13) and, therefore, it possesses three linearly independent eigensolutions, which are only restricted to the exterior surface  $S_0$ .

An idea given by Power [12] for the solution of the deformation of a compressible gas bubble in an arbitrary shear flow, in terms of a well-posed second-kind Fredholm integral equation, will be followed here in order to remove the eigensolutions at each of the bubble surfaces. Let the solution of the present second-kind boundary-value problem be sought in the form of a single-layer potential over the complete surface  $S$  plus  $M$  source harmonic potentials, each of them located at the interior of each of the bubbles enclosed by the viscous drop, *i.e.*

$$u_i(x) = - \int_S u_i^j(x, y)\Phi_j(y) dS_y + \sum_{n=1}^M \frac{\alpha^n(x_i - x_i^n)}{2\pi R_n^2} \quad \text{for every } x \in \Omega \tag{25}$$

with  $R_n = |x_i - x_i^n|$  and  $x_i^n$  the coordinates of a point inside each of the bubbles. The last  $M$  terms represent the velocity field due to the harmonic potentials  $\log(R_n)/2\pi$ , i.e.  $u_i^S = (1/2\pi)\partial \log R_n/\partial x_i$ .

The source strengths are chosen to be linearly dependent upon the single-layer density at the corresponding bubble surface in the following manner:

$$\alpha^n = \int_{S_n} \Phi_i(y)n_i(y) dS_y \quad n = 1, 2, \dots, M. \tag{26}$$

Since the single-layer potential is a regular solution of the Stokes equations in the entire domain with a continuous velocity field across its density-carrying surface, it can be concluded that the net flux due to the volume change of the bubbles is equal to the sum of the strengths  $\alpha^n$  of the sources.

Applying the boundary condition (17) to the flow field defined by Equation (25), using the jump property of the stresses of the single layer, and adding to the surface traction equation at the exterior surface  $S_0$  a term proportional to the rigid body vectors  $\boldsymbol{\varphi}^l, l = 1, 2, 3$ , which as before will be proven not to alter the nature of the problem, we obtain the following system of linear Fredholm integral equations of the second kind:

$$\begin{aligned} \frac{1}{2}\Phi_i(\xi) - \int_{S_0} K_{ji}(y, \xi)\Phi_j(y) dS_y - \int_{S-S_0} K_{ji}(y, \xi)\Phi_j(y) dS_y \\ + \sum_{n=1}^M \alpha^n \sigma_{ij}(\mathbf{u}^{S,n}(\xi))n_j(\xi) + \varphi_i^l(\xi)\beta_l = \gamma\kappa(\xi)n_i(\xi) \quad \text{for } \xi \in S_0, \end{aligned} \tag{27}$$

$$\begin{aligned} -\frac{1}{2}\Phi_i(\xi) - \int_{S_m} K_{ji}(y, \xi)\Phi_j(y) dS_y - \int_{S-S_m} K_{ji}(y, \xi)\Phi_j(y) dS_y \\ + \sum_{n=1}^M \alpha^n \sigma_{ij}(\mathbf{u}^{S,n}(\xi))n_j(\xi) = -\gamma\kappa(\xi)n_i(\xi) \quad \text{for } \xi \in S_m, \end{aligned} \tag{28}$$

where

$$\sigma_{ij}(\mathbf{u}^{S,n}(\xi)) = \sigma_{ij} \left( \frac{(\xi - \xi^n)}{2\pi R_n^2} \right) = \frac{1}{\pi} \left( \frac{\delta_{ij}}{R_n^2} - \frac{2(\xi_i - \xi_i^n)(\xi_j - \xi_j^n)}{R_n^4} \right)$$

and  $\boldsymbol{\beta}$  has been chosen as before:

$$\beta_l = \int_{S_0} \Phi_i \varphi_i^l dS \quad l = 1, 2, 3.$$

The proof that the additional terms in Equation (27), proportional to the rigid body vectors, do not alter the nature of the problem follows from the solvability condition of the present problem, i.e. Equation (18). We may evaluate the total force and torque upon the surface  $S_0$  by multiplying Equation (27) by the rigid body vector,  $\boldsymbol{\varphi}^P$ , at a point on the surface  $S_0(\xi)$  and integrating the resulting expression with respect to  $\xi$ . Using equation (15) and noting that



no contribution is obtained from the potential sources since all harmonic potentials yield zero total forces and torque at any closed surface, we obtain the following equation:

$$-\int_{S-S_0} \Phi_j(y) \varphi_j^P(y) dS_y + \beta_l \int_{S_0} \varphi_i^P(\xi) \varphi_i^l(\xi) dS_\xi = \int_{S_0} \gamma \kappa(\xi) n_i(\xi) \varphi_i^P(\xi) dS_\xi. \quad (29)$$

The property that a double-layer potential with a rigid body vector as density yields an interior flow field that behaves like a rigid body motion, *i.e.*

$$\int_{S_0} K_{ji}(y, \xi) \varphi_i^P(\xi) dS_\xi = \varphi_j^P(y) \quad \text{for every } y \text{ inside } S_0$$

has been used in obtaining Equation (29). For the following analysis, it is important to notice that such double-layer potential is identically equal to zero outside its density-carrying surface.

If Equation (28) is multiplied by the rigid body vector  $\varphi^P$  at a point of the surface  $S_m(\xi)$  and the resulting expression integrated with respect to  $\xi$ , then

$$-\int_{S_m} \Phi_i(\xi) \varphi_i^P(\xi) dS_\xi = -\int_{S_m} \gamma \kappa(\xi) n_i(\xi) \varphi_i^P(\xi) dS_\xi \quad \text{for each } m = 1, 2, \dots, M, \quad (30)$$

where

$$\int_{S_m} K_{ji}(y, \xi) \varphi_i^P(\xi) dS_\xi = 0$$

for every  $y$  outside  $S_m$  as noticed above. Therefore, from (29), the addition of (30) for all  $m$  surfaces, the boundary condition (17) and the solvability condition (18), it follows that

$$\beta_l \int_{S_0} \varphi_i^P(\xi) \varphi_i^l(\xi) dS_\xi = 0.$$

Hence, the vector  $\beta$  has to be identically equal to zero, as in the previous section. A theoretical proof of uniqueness of solution to the system (27–28) is given in Appendix B.

### 3. Numerical procedures

#### 3.1. INDIRECT BOUNDARY-ELEMENT METHOD

The numerical procedures will be first described for the case of a simply-connected domain. Equation (13) can be written in the following discretized form:

$$\begin{aligned} c_{ij}(\xi) \Phi_j(\xi) - \sum_{d=1}^N \Phi_j^k \int_{S_d} K_{ji}(y, \xi) N_k(y) dS_y \\ + \varphi_i^l(\xi) \sum_{d=1}^N \Phi_j^k \int_{S_d} \varphi_j^l(y) N_k(y) dS_y = \gamma \kappa(\xi) n_i(\xi), \end{aligned} \quad (31)$$

where  $N$  is the number of boundary elements and the term  $\beta_l$  has been substituted according to Equation (14). The term  $c_{ij}$  is the characteristic term, given by the expression

$$c_{ij}(\xi) = \frac{1}{2} \delta_{ij}$$

if the surface  $S$  is smooth at  $\xi$ ; otherwise,  $c_{ij}$  is given by:

$$c_{ij}(\xi) = \frac{\Delta\varphi}{2\pi}\mathbf{I} + \frac{1}{2\pi}\{\mathbf{J}(\varphi_i) - \mathbf{J}(\varphi_2)\}, \quad (32)$$

where  $\varphi_1$  and  $\varphi_2$  are the angles subtended between the  $x_1$ -axis and the tangents  $t_1$  and  $t_2$  at point  $\xi$ , and  $\Delta\varphi$  is the angle subtended between the tangents to two contiguous nodes [20, p. 113].  $\mathbf{I}$  is the identity matrix, and  $\mathbf{J}(\varphi)$  is equal to:

$$\mathbf{J}(\varphi) = \begin{bmatrix} \sin 2\varphi_2 - \sin 2\varphi_1 & \cos 2\varphi_2 - \cos 2\varphi_1 \\ \cos 2\varphi_2 - \cos 2\varphi_1 & \sin 2\varphi_1 - \sin 2\varphi_2 \end{bmatrix}.$$

In this work, quadratic boundary elements are used in all simulations. Adding up those terms in Equation (31) multiplying the same nodal value  $\Phi_j^k$ , we have the coefficients:

$$h_{ij,\xi d}^k = - \int_{S_d} K_{ji}(y, \xi) N_k(y) dS_y + \varphi_i^l(\xi) \int_{S_d} \varphi_j^l(y) N_k(y) dS_y.$$

The above integrals are all carried out numerically by use of Gauss quadrature [21]. Equation (31) for a collocation point  $\xi$  can then be expressed in the form:

$$\sum_{\chi=1}^P \mathbf{H}_{\xi\chi} \Phi_{\chi} = \mathbf{T}_{\xi} \quad (33)$$

with

$$\mathbf{H}_{\xi\chi} = \hat{\mathbf{H}}_{\xi\chi} + \delta_{\xi\chi} \mathbf{c}_{\xi},$$

where  $\delta_{\xi\chi}$  is the Kronecker delta,  $\mathbf{c}_{\xi}$  is a  $2 \times 2$  matrix, each  $\hat{\mathbf{H}}_{\xi n}$  is a  $2 \times 2$  matrix obtained by assembling the coefficients  $h_{ij,\xi d}^k$  and each  $\Phi_n$  is a vector with components  $\Phi_1, \Phi_2$ ;  $P$  is the total number of boundary nodes. The vector  $\mathbf{T}$  represents the surface tension, *i.e.*

$$T_i(\xi) = \gamma \kappa(\xi) n_i(\xi).$$

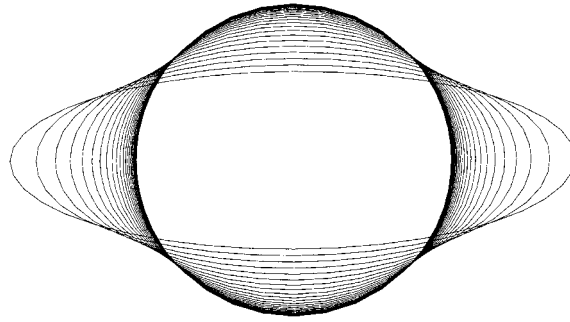
Equation (33) is applied at each node generating a  $2P \times 2P$  system of equations which can be expressed in matrix form as:

$$\mathbf{H}\Phi = \mathbf{T}. \quad (34)$$

The above system of equations for the vector density  $\Phi$  was solved by Gauss elimination. The calculated values of  $\Phi$  are then used to find the boundary velocities from Equation (8) which is also valid at boundary points since the single-layer potential  $u_i^j(\xi, y)$  is continuous across the density-carrying surface  $S$ .

For multiply-connected domains, the discretized form of Equations (27) and (28) is obtained following a similar procedure as for simply-connected domains. The coefficients multiplying the same nodal value  $\Phi_j^k$  are added up as follows:

$$h_{ij,\xi d}^k = - \int_{S_d} K_{ji}(y, \xi) N_k(y) dS_y + \sum_{n=1}^M \sigma_{il}(\mathbf{u}^{S,n}(\xi)) n_l(\xi) \int_{(S_n)d} N_k(y) n_j(y) dS_y + \varphi_i^l(\xi) \int_{(S_0)d} \varphi_j^l(y) N_k(y) dS_y$$



$t=0.0(0.1)10.0$

Figure 2. Deformation of an ellipse into a circle due to surface tension.

in which the last term is included only when  $\xi \in S_0$ . The matrix assembly, solution of the final system of equations, and calculation of boundary velocities are carried out as previously described.

#### 4. Results and discussion

A computer program was written based on the developed integral-equation formulations. The physical parameters were made dimensionless, following Kuiken [1], by defining a characteristic velocity  $u_c$ , a characteristic pressure  $p_c$  and a characteristic time  $t_c$ :

$$u_c = \frac{\gamma}{\mu}, \quad p_c = \frac{\gamma}{l}, \quad t_c = \frac{l\mu}{\gamma}, \quad (35)$$

where  $l$  is a characteristic length.

The surface deformations are calculated by a simple Euler scheme in which the displacement of each fluid particle is found by simply multiplying its computed velocity by the time step. This scheme provided sufficient accuracy for all cases studied herein.

##### 4.1. SIMPLY-CONNECTED DOMAINS

A simply-connected viscous fluid region of arbitrary shape subjected to surface tension will deform until a circular form is achieved, since the normal component of the stress tensor is constant when the curvature is constant along the surface  $S$ . As the fluid is assumed to be incompressible, the area of the region should be conserved at all times.

Kuiken [1] studied the deformation of an elliptical flow region ( $x^2 + 10y^2 = 1$ ) due to surface tension. The steady-state circular shape was achieved at a dimensionless time of  $t = 10$ . A similar deformation process can be seen in Figure 2, obtained from the present formulation with 20 quadratic elements evenly distributed on the elliptical boundary, with deformations calculated at time steps of  $\Delta t = 0.1$ . Table 1 shows coordinates of nodal points on the first quadrant of the ellipse at times  $t = 0, 2, 5$  and 10, indicating that the generated values for  $t = 10$  indeed belong to a circle of radius approximately equal to 0.557. The table also shows that there is no significant difference between results for  $t = 5$  and  $t = 10$ .

The present formulation also produced acceptable values for the area conservation. The initial ellipse has an area  $\pi ab = 0.9934$  while the final circular area is  $\pi r^2 = 0.9747$ , which

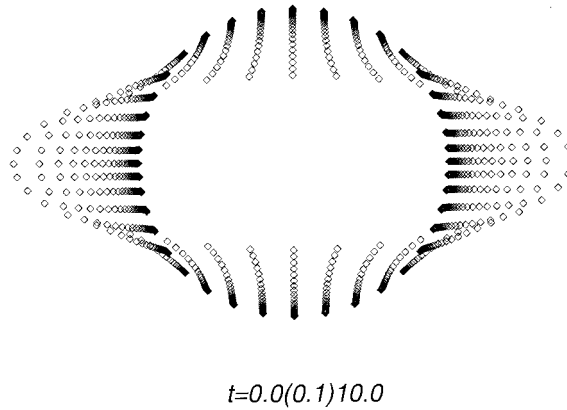


Figure 3. Direction of motion for points on the surface of the ellipse.

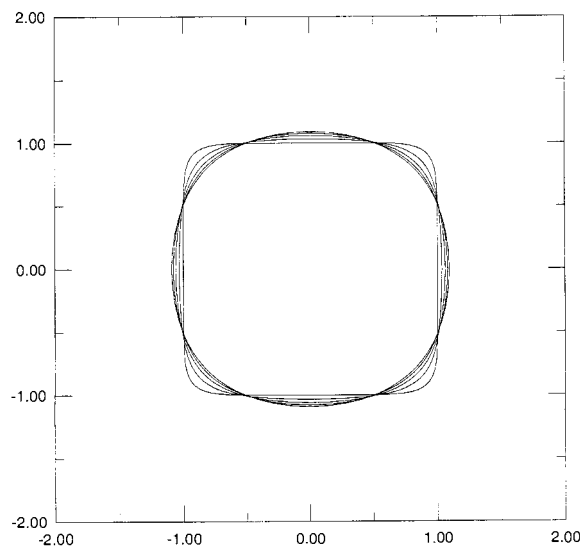


Figure 4. Deformation of square with rounded-off corners under action of surface tension.

is 1.88% smaller. Using the same discretization of 20 quadratic elements, but reducing the time step size improves area conservation. For  $\Delta t = 0.01$ , the radius of the final circular form is 0.5617, its area 0.9912 and the error 0.22%; for  $\Delta t = 0.001$ , the radius is 0.5622, the area 0.9929 and the error 0.05%. Keeping the time step constant and doubling the number of elements produced virtually no improvement in the results.

Another interesting result from Kuiken's paper refers to the evolution of particles on the surface of the elliptical curve with time. The node displacement of Figure 3 shows a similar behaviour to that of Kuiken [1].

The next example was taken from Kuiken [2] and van de Vorst *et al.* [3] and consists of a square with rounded-off corners. The present formulation was applied to the same case and results can be seen in Figure 4. Table 2 shows coordinates of nodal points on the first quadrant of Figure 4 at  $t = 0$ , together with the results of van de Vorst *et al.* [3] and the completed indirect BEM for  $t = 1$ . Very good agreement between both simulations can be observed. A

Table 1. Nodal coordinates of points in the first quadrant of Figure 2.

Nodes	$t = 0.0$		$t = 2.0$		$t = 5.0$		$t = 10.0$	
	$x_i$	$y_i$	$x_i$	$y_i$	$x_i$	$y_i$	$x_i$	$y_i$
1	1.0000	0.0000	0.5647	0.0000	0.5568	0.0000	0.5569	0.0000
2	0.9877	0.0495	0.5626	0.0474	0.5547	0.0486	0.5546	0.0508
3	0.9511	0.0977	0.5550	0.1016	0.5472	0.1032	0.5467	0.1061
4	0.8910	0.1436	0.5378	0.1675	0.5301	0.1705	0.5285	0.1756
5	0.8090	0.1859	0.5081	0.2397	0.5013	0.2425	0.4995	0.2464
6	0.7071	0.2236	0.4619	0.3161	0.4556	0.3202	0.4523	0.3250
7	0.5878	0.2558	0.3981	0.3896	0.3937	0.3940	0.3907	0.3969
8	0.4540	0.2818	0.3168	0.4548	0.3133	0.4605	0.3097	0.4629
9	0.3090	0.3008	0.2204	0.5057	0.2185	0.5124	0.2159	0.5134
10	0.1564	0.3123	0.1131	0.5382	0.1121	0.5457	0.1105	0.5459
11	0.0000	0.3162	0.0000	0.5493	0.0000	0.5571	0.0000	0.5570

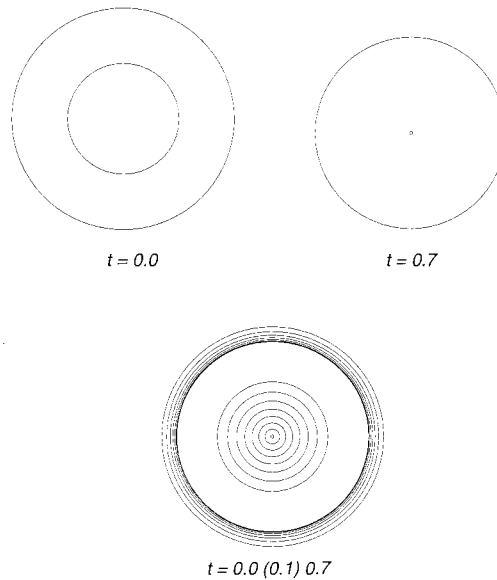


Figure 5. Shrinkage of a fluid disk with a circular hole centered at its origin.

constant time step of  $\Delta t = 0.01$ , as used by van de Vorst *et al.* [3], has also been adopted here.

#### 4.2. MULTIPLY-CONNECTED DOMAINS

The simplest example of a multiply-connected domain is the case of a circular disc containing a circular hole. Because of surface tension acting on the outer boundary, the total region shrinks due to the vanishing of the hole. As the region is circular, with a circular hole centered at its origin, the forces acting on the boundary are constant and the shrinkage will also be constant. The deformation will cease when the hole vanishes.

Table 2. Nodal coordinates of points in the first quadrant of Figure 4.

Nodes	$t = 0.0$		$t = 1.0$ (van de Vorst <i>et al.</i> [3])		$t = 1.0$ (present results)	
	$x_i$	$y_i$	$x_i$	$y_i$	$x_i$	$y_i$
1	1.00000	0.00000	1.09161	0.00000	1.09187	0.00000
2	1.00000	0.16245	1.08428	0.15260	1.08451	0.15254
3	0.99999	0.30312	1.06562	0.28334	1.06581	0.28324
4	0.99986	0.42793	1.03877	0.39705	1.03895	0.39691
5	0.99910	0.53967	1.00569	0.49609	1.00587	0.49593
6	0.99648	0.63905	0.96833	0.58120	0.96857	0.58090
7	0.99006	0.72552	0.92909	0.65244	0.92939	0.65206
8	0.97809	0.79675	0.89136	0.70909	0.89176	0.70864
9	0.96009	0.85215	0.85749	0.75269	0.85776	0.75248
10	0.93751	0.89268	0.82837	0.78582	0.82879	0.78549
11	0.91239	0.92146	0.80304	0.81192	0.80331	0.81178
12	0.88350	0.94365	0.77784	0.83573	0.77798	0.83568
13	0.84613	0.96262	0.74768	0.86174	0.74787	0.86158
14	0.79517	0.97847	0.70764	0.89259	0.70753	0.89259
15	0.72904	0.98966	0.65509	0.92771	0.65501	0.92762
16	0.64666	0.99613	0.58741	0.96553	0.58732	0.96540
17	0.54956	0.99896	0.50456	1.00271	0.50455	1.00253
18	0.43814	0.99983	0.40611	1.03649	0.40608	1.03633
19	0.31187	0.99999	0.29130	1.06442	0.29129	1.06429
20	0.16690	1.00000	0.15672	1.08419	0.15670	1.08412
21	0.00000	1.00000	0.00000	1.09191	0.00000	1.09165

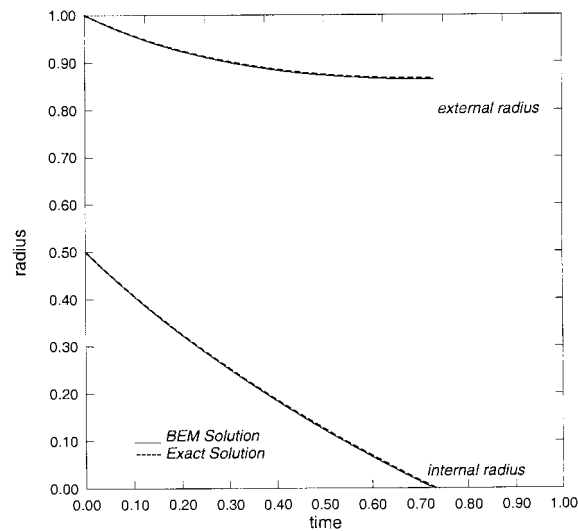


Figure 6. Shrinkage of a fluid disk with a circular hole centered at its origin: Comparison between exact and numerical solutions for the inner and outer radii.

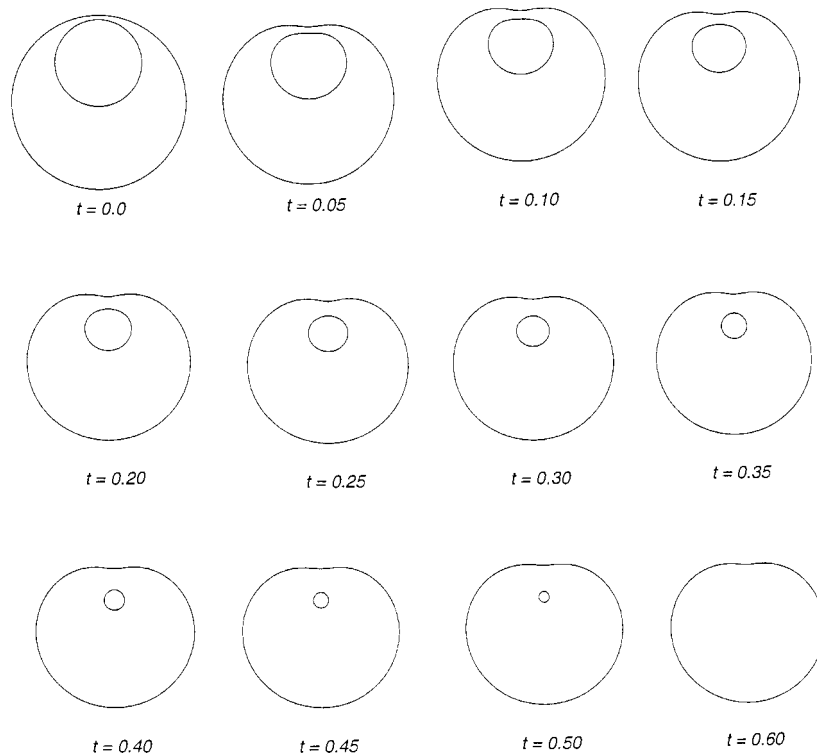


Figure 7. Shrinkage of a circular hole located near the boundary of a circular fluid disk. The hole shrinks remaining inside the disk.

For the case of a fluid region of initial radius  $R_o$  containing a circular hole of initial radius  $R_i$  centered at its origin, the final radius  $R_f$  of the circular fluid region after deformation is easily found analytically. Using the same nondimensional data as in van de Vorst [22], for an initial exterior radius of  $R_o = 1$  and an initial interior radius of  $R_i = 0.5$ , we find a final radius  $R_f$  that is equal to  $\sqrt{0.75} \approx 0.866$ . The numerical value found with the present simulation was  $R_f \approx 0.864$ , which is 0.2% smaller than the exact value. The time when the hole vanishes can also be found analytically, and van de Vorst [22] has shown it to be  $t \approx 0.73$ ; we obtained exactly the same value by using the present BEM formulation with a discretization of 32 quadratic elements, 16 along each surface.

Figure 5 shows the vanishing of the circular hole inside the circular fluid disk. Using a time step of  $\Delta t = 0.01$  for the analysis, curves are plotted from  $t = 0$  to  $t = 0.7$  at steps of  $t = 0.1$ . A very good agreement was achieved with the results of van de Vorst [22]. Figure 6 shows the time variation of the outer/inner radii of the fluid disk depicted in Figure 5, for the numerical and analytical solutions. The results are practically coincident, confirming the accuracy of the graphs in the previous figure.

Another case reported by van de Vorst [22] is that of a circular fluid disk with a circular hole located near the disk boundary. An interesting question regarding the motion is whether the hole would deform towards the boundary, turning the disk into a simply-connected domain. As shown by van de Vorst [22], the circular hole shrinks, but remains in the fluid region all the time. The results obtained with the present formulation, depicted in Figure 7, are in close

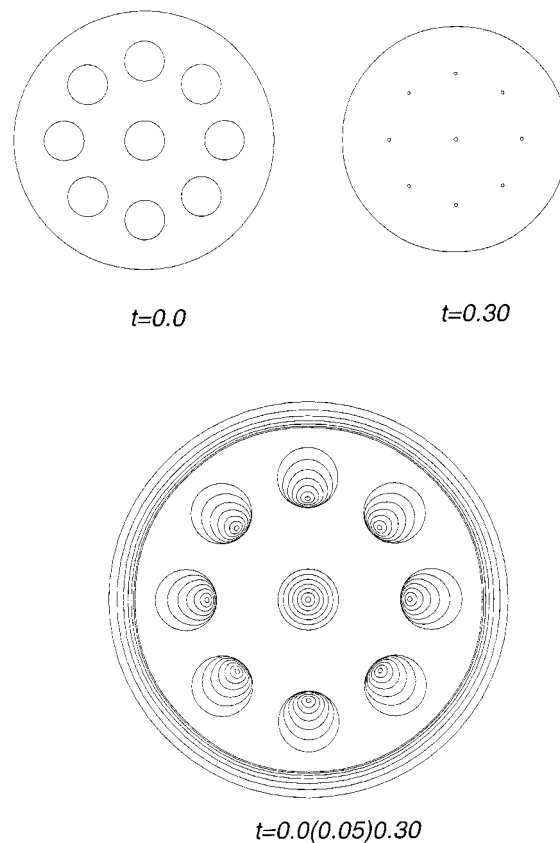


Figure 8. Shrinkage of a fluid disk with 9 equally-sized cylindrical pores.

visual agreement with van de Vorst's results for the same nondimensional data: fluid disk radius of 1; initial hole radius of 0.5 with midpoint of the hole at  $y = 0.45$ .

The deformation of a fluid cylinder with 9 cylindrical pores can be seen in Figure 8. The calculations were carried out with the same nondimensional values used by van de Vorst [22]: radius of the cylinder equal to 1.3 and radius of each pore equal to 0.2. The shrinkage was calculated at time steps of  $\Delta t = 0.01$  and shown at steps of  $\Delta t = 0.05$ . As can be seen in Figure 8, the holes have almost vanished at  $t = 0.3$ .

## 5. Conclusions

In this paper a new integral equation formulation has been presented, in terms of only one surface potential, which provides unique solutions to problems involving the deformation of a bounded region of slow viscous flow, with or without air bubbles, subject to surface tension. The formulation has been verified by application to viscous sintering problems. Numerical results displayed excellent agreement with previous results available in the literature.

The formulation is general and can be extended to sintering problems with fluid impurities or solid inclusions [23]. We advocate using an indirect boundary-integral formulation since it provides simpler and more rigorous mathematical analyses of the existence and uniqueness of solution of the resulting Fredholm integral equations. The system of equations generated by



indirect formulations is very stable and more amenable to fast iterative solvers using multipole expansions, without the need of any preconditioning [24].

The formulation affords a simple computational implementation, requiring only extra regular integrations which are computed simultaneously with the standard integrations of the indirect boundary-element scheme. Therefore, the additional computing time for the completed formulation is negligible.

### Appendix A: Proof of uniqueness of solution for simply-connected regions

In order to show that Equation (13) possesses a unique continuous solution  $\Phi$  for a continuous datum  $\gamma\kappa n$  it is sufficient, according to the Fredholm alternative, to show that its homogeneous form

$$\frac{1}{2}\Phi_i^o(\xi) - \int_S K_{ji}(y, \xi)\Phi_j^o(y) dS_y + \varphi_i^l(\xi)\beta_l^o = 0, \quad (\text{A1})$$

where

$$\beta_l^o = \int_S \varphi_i^l \Phi_i^o dS,$$

admits only the trivial solution in the space of continuous functions.

Equation (A1) can be rewritten as

$$\frac{1}{2}\Phi_i^o(\xi) - \int_S K_{ji}(y, \xi)\Phi_j^o(y) dS_y = -\beta_l^o \varphi_i^l(\xi). \quad (\text{A2})$$

As in the case of Equation (11), the above equation has a solution if and only if the nonhomogeneous term,  $-\beta^o \varphi^l$ , is orthogonal to the rigid body vectors, *i.e.*

$$\beta_l^o \int_S \varphi_i^l(\xi)\varphi_i^n(\xi) dS_\xi = 0, \quad l, n = 1, 2, 3.$$

Consequently, and similarly to Equation (16), it is found from the above equation that  $\beta^o \equiv 0$ . Therefore, Equation (A1) reduces to the homogeneous form of Equation (11), which possesses three linearly-independent eigensolutions,  $\Psi^n$ ,  $n = 1, 2, 3$ . From the above analysis it follows that

$$\beta_l^o = \int_S \varphi_i^l \Phi_i^o dS = \int_S \varphi_i^l \Psi_i^n dS = 0, \quad l, n = 1, 2, 3. \quad (\text{A3})$$

As follows from the homogeneous form of Equation (11), a single-layer potential  $V(x, \Psi^n)$ ,  $n = 1, 2, 3$ , coming from the domain interior to  $S$ , has to yield a zero surface traction on  $S$ . Then, the single-layer potential  $V(x, \Psi^n)$  represents an interior Stokes flow moving as a rigid body,  $\varphi^l$ , with a zero associated pressure. From the continuity property of the velocity field of a single-layer potential across its density-carrying surface, it is concluded that the limiting value of such single-layer potential, as  $x$  approaches a point  $\xi \in S$  from the outside of  $S$ , is also  $\varphi^l$ . On the other hand, from the discontinuity property of the surface traction of a single-layer potential across its density-carrying surface and the homogeneous form of Equation (11), it follows that the limiting value of the surface traction on  $S$ , of such single-layer potential coming from the exterior domain, has to be equal to  $\Psi^n$ .

Equation (A3) states that the total force and torque exerted upon the surface  $S$  by the exterior flow field defined by the single-layer potential  $\mathbf{V}(x, \Psi^n)$  have to be identically equal to zero. But, according to Chang and Finn's [25] interpretation of the Stokes paradox, this is not possible since such flow field represents the fluid motion exterior to the surface  $S$  due to the motion of the surface  $S$  as a rigid body, and having a logarithmic behaviour at infinity. Therefore, such flow field always yields a nonzero total force. Hence, if Equation (A3) is satisfied, the flow field due to the single-layer potential  $\mathbf{V}(x, \Phi^o)$ , with  $\Phi^o$  as any nontrivial solution of Equation (A1), has to be the null field in the domain exterior to the surface  $S$ . From the continuity property of the single-layer potential across its density-carrying surface, it follows that  $\mathbf{V}(x, \Phi^o)$  represents a null flow field in the entire space; hence, by the discontinuity property of the surface traction of such single-layer potential, it is concluded that  $\Phi^o \equiv 0$  on  $S$ . In this way, it is shown that the addition to the original integral equation of the term proportional to the rigid body motion does not alter the nature of the original problem, and that the deficient range of the original integral operator is thus removed.

It was, therefore, established that the nonhomogeneous integral Equation (13) has a unique continuous solution  $\Phi$  for any continuous datum, which satisfies the solvability condition of the present interior second-kind boundary-value problem. It was also established that the Stokes velocity field given by Equation (8), with this  $\Phi$  as density, together with its corresponding pressure field, provides the unique solution to the problem described by Equations (1), (2) and (3).

From the previous analysis, it follows that the addition of the term  $\varphi^l \beta_l^o$  to the homogeneous integral equation

$$\frac{1}{2} \Phi_i^o(\xi) - \lambda \int_S K_{ji}(y, \xi) \Phi_j^o(y) dS_y = 0 \tag{A4}$$

removed its eigenvalue at  $\lambda = 1$ . Equation (A4) is known to possess only two eigenvalues,  $\lambda = 1$  and  $\lambda = -1$ , on the complex disk  $|\lambda| \leq 1$  (see Power [7] and Pozrikidis [26]). Therefore, the analytical solution of Equation (13) can be found in terms of a modified Neumann series as defined by Goursat [27].

### Appendix B: Proof of uniqueness of solution for multiply-connected regions

Proceeding as before, in order to guarantee that the system (27–28) possesses a unique continuous solution  $\Phi$ , we must prove that the following system of homogeneous integral equations admits only the trivial solution,

$$\begin{aligned} & \frac{1}{2} \Phi_i^o(\xi) - \int_{S_0} K_{ji}(y, \xi) \Phi_j^o(y) dS_y - \int_{S-S_0} K_{ji}(y, \xi) \Phi_j^o(y) dS_y \\ & + \sum_{n=1}^M \alpha^{o^n} \sigma_{ij}(\mathbf{u}^{S,n}(\xi)) n_j(\xi) + \varphi_i^l(\xi) \beta_l^o = 0 \quad \text{for } \xi \in S_0, \end{aligned} \tag{B1}$$

$$\begin{aligned} & -\frac{1}{2} \Phi_i^o(\xi) - \int_{S_m} K_{ji}(y, \xi) \Phi_j^o(y) dS_y - \int_{S-S_m} K_{ji}(y, \xi) \Phi_j^o(y) dS_y \\ & + \sum_{n=1}^M \alpha^{o^n} \sigma_{ij}(\mathbf{u}^{S,n}(\xi)) n_j(\xi) = 0 \quad \text{for } \xi \in S_m \end{aligned} \tag{B2}$$

with  $m = 1, 2, \dots, M$ . Here

$$\alpha^{\sigma^n} = \int_{S_n} \Phi_i^{\sigma}(y) n_i(y) dS_y, \quad n = 1, 2, \dots, M \quad (\text{B3})$$

and

$$\beta_l^{\sigma} = \int_{S_0} \Phi_i^{\sigma}(y) \varphi_i^l(y) dS_y. \quad (\text{B4})$$

From the previous analysis it follows that the additional term in equation (B1) has to be equal to zero, *i.e.*

$$\beta_l^{\sigma} = \int_{S_0} \Phi_i^{\sigma}(y) \varphi_i^l(y) dS_y \equiv 0. \quad (\text{B5})$$

From Equations (B1) and (B2), with  $\beta^{\sigma} = 0$ , it also follows that the flow field in the bounded domain  $\Omega$ , defined by a single-layer potential with density given by any nontrivial solution of (B1) and (B2) plus the sum of the corresponding harmonic sources, has to be equal to a rigid body motion as its velocity field and zero pressure. Therefore, the following vector fields  $V^1$  and  $V^2$  defined below are equal in  $\Omega$ :

$$V_i^1 = - \int_S u_i^j(x, y) \Phi_j^{\sigma}(y) dS_y - \varphi_i^l(x), \quad (\text{B6})$$

$$V_i^2 = - \sum_{n=1}^M \alpha^{\sigma^n} u_i^S(x). \quad (\text{B7})$$

On the other hand,  $V^1$  yields zero flux across any closed surface and  $V^2$  yields a total flux equal to  $\alpha^{\sigma^n}$  in each of the internal closed surfaces  $S_n$ ,  $n = 1, 2, \dots, M$ . Therefore, according to the identity of  $V^1$  and  $V^2$ ,

$$\alpha^{\sigma^n} = \int_{S_n} \Phi_i^{\sigma}(y) n_i(y) dS_y = 0. \quad (\text{B8})$$

From (B5) and (B8), it results that the system (B1–B2) reduces to the system (19–20), and therefore it possesses  $M + 3$  linearly-independent eigensolutions. However, the  $M$  interior eigensolutions  $\Phi_i^{\sigma}(\xi) = C n_i(\xi)$  are removed by condition (B8), and Equation (19) is then reduced to the adjoint of Equation (12) whose three eigensolutions are removed by Equation (B5), according to Equation (A3). Therefore, the only solution of the system (B1–B2) is the trivial solution.

Let us consider, for simplicity, the case of a single internal surface. In this case, Equations (B1) and (B2) reduce to:

$$\begin{aligned} \frac{1}{2} \Phi_i^{\sigma}(\xi) - \int_{S_0} K_{ji}(y, \xi) \Phi_j^{\sigma}(y) dS_y - \int_{S_1} K_{ji}(y, \xi) \Phi_j^{\sigma}(y) dS_y \\ + \alpha^{\sigma} \sigma_{ij}(\mathbf{u}^{S_1}(\xi)) n_j(\xi) + \varphi_i^l(\xi) \beta_l^{\sigma} = 0 \quad \text{for } \xi \in S_0, \end{aligned} \quad (\text{B9})$$

$$\begin{aligned} -\frac{1}{2} \Phi_i^{\sigma}(\xi) - \int_{S_1} K_{ji}(y, \xi) \Phi_j^{\sigma}(y) dS_y - \int_{S_0} K_{ji}(y, \xi) \Phi_j^{\sigma}(y) dS_y \\ + \alpha^{\sigma} \sigma_{ij}(\mathbf{u}^{S_1}(\xi)) n_j(\xi) = 0 \quad \text{for } \xi \in S_1. \end{aligned} \quad (\text{B10})$$

From the previous analysis, it follows that the added terms remove the eigenvalues  $\lambda_0 = 1$  and  $\lambda_1 = 1$  of the following system of homogeneous equations:

$$\frac{1}{2}\Phi_i^o(\xi) - \lambda_0 \int_{S_0} K_{ji}(y, \xi)\Phi_j^o(y) dS_y - \lambda_1 \int_{S_1} K_{ji}(y, \xi)\Phi_j^o(y) dS_y = 0 \quad \text{for } \xi \in S_0, \quad (\text{B11})$$

$$\begin{aligned} & -\frac{1}{2}\Phi_i^o(\xi) - \lambda_1 \int_{S_1} K_{ji}(y, \xi)\Phi_j^o(y) dS_y \\ & - \lambda_0 \int_{S_0} K_{ji}(y, \xi)\Phi_j^o(y) dS_y = 0 \quad \text{for } \xi \in S_1. \end{aligned} \quad (\text{B12})$$

According to the Fredholm alternative, if  $\lambda_0$  and  $\lambda_1$  are eigenvalues of the above system, then  $\overline{\lambda_0}$  and  $\overline{\lambda_1}$  are eigenvalues of the adjoint system

$$\frac{1}{2}\Psi_i^o(\xi) - \overline{\lambda_0} \int_{S_0} K_{ij}(\xi, y)\Psi_j^o(y) dS_y - \overline{\lambda_1} \int_{S_1} K_{ij}(\xi, y)\Psi_j^o(y) dS_y = 0 \quad \text{for } \xi \in S_0, \quad (\text{B13})$$

$$\begin{aligned} & -\frac{1}{2}\Psi_i^o(\xi) - \overline{\lambda_1} \int_{S_1} K_{ij}(\xi, y)\Psi_j^o(y) dS_y \\ & - \overline{\lambda_0} \int_{S_0} K_{ij}(\xi, y)\Psi_j^o(y) dS_y = 0 \quad \text{for } \xi \in S_1. \end{aligned} \quad (\text{B14})$$

Let us now define an auxiliary double-layer potential flow field in the form:

$$U_i^1(x) = \int_{S_0} K_{ij}(x, y)\Psi_j(y) dS_y + \frac{\overline{\lambda_1}}{\lambda_0} \int_{S_1} K_{ij}(x, y)\Psi_j(y) dS_y. \quad (\text{B15})$$

This is a complex function, *i.e.*  $U^1(x) = U^{1r}(x) + iU^{1i}(x)$ , whose real and imaginary parts both satisfy the Stokes equations. It has a discontinuous velocity and continuous tractions across the surfaces  $S_0$  and  $S_1$ . In particular, across the surface  $S_0$  we have:

$$U_i^1(\xi)_{(i)} = \frac{1}{2}\Psi_i(\xi) + \int_{S_0} K_{ij}(\xi, y)\Psi_j(y) dS_y + \frac{\overline{\lambda_1}}{\lambda_0} \int_{S_1} K_{ij}(\xi, y)\Psi_j(y) dS_y, \quad (\text{B16})$$

$$U_i^1(\xi)_{(e)} = -\frac{1}{2}\Psi_i(\xi) + \int_{S_0} K_{ij}(\xi, y)\Psi_j(y) dS_y + \frac{\overline{\lambda_1}}{\lambda_0} \int_{S_1} K_{ij}(\xi, y)\Psi_j(y) dS_y. \quad (\text{B17})$$

In the above,  $U^1(\xi)_{(i)}$  is the limiting value of  $U^1(x)$  when a point  $x$  tends to a point  $\xi \in S_0$  coming from the domain interior to  $S_0$ , and  $U^1(\xi)_{(e)}$  is the limiting value at  $\xi$  coming from the domain exterior to  $S_0$ . The above formulae allow us to transform Equation (B13) to the form

$$[U_i^1(\xi)_{(i)} - U_i^1(\xi)_{(e)}] - \overline{\lambda_0}[U_i^1(\xi)_{(i)} + U_i^1(\xi)_{(e)}] = 0$$

for every  $\xi \in S_0$ , or

$$(1 - \overline{\lambda_0})U_i^1(\xi)_{(i)} = (1 + \overline{\lambda_0})U_i^1(\xi)_{(e)}. \quad (\text{B18})$$

Multiplying the above equation by the surface traction, at  $S_0$ , of the flow field conjugate to  $\mathbf{U}^1(x)$ , *i.e.*  $\mathbf{U}^{1*}(x) = \mathbf{U}^{1r}(x) - i\mathbf{U}^{1i}(x)$ , and integrating the resulting expression over the surface  $S_0$ , we obtain

$$\begin{aligned} & \int_{S_0} [U_i^{1r} \sigma_{ij}(\mathbf{U}^{1r})n_j + U_i^{1i} \sigma_{ij}(\mathbf{U}^{1i})n_j]_{(i)} dS \\ &= \frac{1 + \overline{\lambda_0}}{1 - \overline{\lambda_0}} \int_{S_0} [U_i^{1r} \sigma_{ij}(\mathbf{U}^{1r})n_j + U_i^{1i} \sigma_{ij}(\mathbf{U}^{1i})n_j]_{(e)} dS. \end{aligned} \quad (\text{B19})$$

In obtaining the above equation, use was made of the continuity property of the surface traction of the double-layer potential across its density-carrying surface and Lorentz's reciprocal theorem [5]

$$\int_{S_0} [U_i^{1r} \sigma_{ij}(\mathbf{U}^{1i})n_j - U_i^{1i} \sigma_{ij}(\mathbf{U}^{1r})n_j] dS = 0.$$

From Green's first formula for the Stokes equations, it follows that the first integral in Equation (B19) is real and positive, while the second integral is real but negative. Therefore, such a relation is only possible if the coefficient  $(1 + \overline{\lambda_0})/(1 - \overline{\lambda_0})$  is real and negative. This implies that the eigenvalue  $\overline{\lambda_0}$  has to be real, *i.e.*  $\overline{\lambda_0} = \lambda_0$ , and that  $|\lambda_0| > 1$ .

Similarly, if we define the auxiliary Stokes flow

$$U_i^2(x) = \int_{S_1} K_{ij}(x, y)\Psi_j(y) dS_y + \frac{\overline{\lambda_0}}{\lambda_1} \int_{S_0} K_{ij}(x, y)\Psi_j(y) dS_y, \quad (\text{B20})$$

we find that Equation (B14) can be written in the form

$$[U_i^2(\xi)_{(i)} - U_i^2(\xi)_{(e)}] + \overline{\lambda_1}[U_i^2(\xi)_{(i)} + U_i^2(\xi)_{(e)}] = 0$$

for every  $\xi \in S_1$ . Following the same approach as before, it is found that the eigenvalue  $\overline{\lambda_1}$  has to be real, *i.e.*  $\overline{\lambda_1} = \lambda_1$ , and that  $|\lambda_1| > 1$ .

It can then be concluded that the system of Equations (B11) and (B12) has no eigenvalues in the interior of the complex disks  $|\lambda_0| \leq 1$  and  $|\lambda_1| \leq 1$ , and that the eigenvalue at  $\lambda_0 = \lambda_1 = 1$  was removed by the additional terms in Equations (B9) and (B10). As for the case of simply-connected regions, the analytical solution of the system (27) and (28) can be given in terms of the corresponding modified Neumann series [27].

## References

1. H. K. Kuiken, Viscous sintering: the surface-tension-driven flow of a liquid form under the influence of curvature gradients at its surface. *J. Fluid Mech.* 214 (1990) 503–515.
2. H. K. Kuiken, Deforming surfaces and viscous sintering. In: D. G. Dritschel and R. J. Perkins (eds), *The Mathematics of Deforming Surfaces*. Oxford: Clarendon Press (1996) 75–97.
3. G. A. L. van de Vorst, R. M. M. Mattheij and H. K. Kuiken, A boundary element solution for two-dimensional viscous sintering. *J. Comp. Phys.* 100 (1992) 50–63.
4. G. A. L. van de Vorst and R. M. M. Mattheij, Numerical analysis of a two-dimensional viscous sintering problem with non-smooth boundaries. *Computing* 49 (1992) 239–263.
5. H. A. Lorentz, A general theorem on the motion of a fluid with friction and a few results derived from it (in Dutch). *Versl. Acad. Wetensch* 5 (1896) 168–175. Translated and reprinted by H. K. Kuiken, *J. Eng. Math.* 30 (1996) 19–24.

6. H. Power and G. Miranda, Second kind integral equation formulation of Stokes flows past a particle of arbitrary shape. *SIAM J. Appl. Math.* 47 (1987) 689–698.
7. H. Power, Second kind integral equation solution of Stokes flows past  $n$  bodies of arbitrary shape. In: C. A. Brebbia, W. L. Wendland and G. Kuhn (eds), *Boundary Elements IX*, Vol. 3. Berlin: Springer-Verlag (1987) 477–488.
8. S. J. Karrila, Y. O. Fuentes and S. Kim, Parallel computational strategies for hydrodynamic interactions between rigid particles of arbitrary shape in a viscous fluid. *J. Rheology* 33 (1989) 913–947.
9. H. Power and G. Miranda, Integral equation formulation for the creeping flow of an incompressible viscous fluid between two arbitrary closed surfaces, and a possible mathematical model for the brain fluid dynamics. *J. Math. Anal. Appl.* 137 (1989) 1–16.
10. S. J. Karrila and S. Kim, Integral equations of the second kind for Stokes flow: direct solution for physical variables and removal of inherent accuracy limitations. *Chem. Eng. Commun.* 82 (1989) 123–161.
11. H. Power, Matched-asymptotic analysis of low Reynolds number flow past a cylinder of arbitrary cross-sectional shape. *Math. Appl. Comp.* 9 (1990) 111–122.
12. H. Power, The low Reynolds number deformation of a gas bubble in shear flow: a general approach via integral equations. *Eng. Anal. with Boundary Elements* 16 (1992) 61–74.
13. H. Power, The completed double layer boundary integral equation method for two-dimensional Stokes flow. *IMA J. Appl. Math.* 51 (1993) 123–145.
14. S. G. Mikhlin, *Integral Equations and their Application to Certain Problems in Mechanics, Mathematical Physics and Technology*. London: Pergamon Press (1957) 338pp.
15. S. Kim and S. J. Karrila, *Microhydrodynamics: Principles and Selected Applications*. London: Butterworth-Heinemann (1991) 507pp.
16. C. Pozrikidis, *Boundary Integral and Singularity Methods for Linearized Viscous Flow*. Cambridge: Cambridge University Press (1992) 259pp.
17. H. Power and L. C. Wrobel, *Boundary Integral Methods in Fluid Mechanics*. Southampton: Computational Mechanics Publications (1995) 330pp.
18. O. A. Ladyzhenskaya, *The Mathematical Theory of Viscous Incompressible Flow*. New York: Gordon and Breach (1963) 185pp.
19. R. Courant and D. Hilbert, *Methods of Mathematical Physics*. London: Interscience (1992) Vol. 2, 830pp.
20. F. Hartmann, *Introduction to Boundary Elements*. Berlin: Springer-Verlag (1989) 416pp.
21. C. A. Brebbia, J. C. F. Telles and L. C. Wrobel, *Boundary Element Techniques*. Berlin: Springer-Verlag (1984) 464pp.
22. G. A. L. van de Vorst, Integral method for a two-dimensional Stokes flow with shrinking holes applied to viscous sintering. *J. Fluid Mech.* 257 (1993) 667–689.
23. A. R. M. Primo, *Novel Boundary Integral Formulations for Slow Viscous Flow with Moving Boundaries*, Ph.D. Thesis, Brunel University, UK (1998) 169pp.
24. J. E. Gómez and H. Power, A multipole direct and indirect BEM for two-dimensional cavity flow at low Reynolds number. *Eng. Anal. with Boundary Elements* 19 (1997) 17–31.
25. I. D. Chang and R. Finn, On the solution of a class of equations occurring in continuum mechanics, with application to the Stokes paradox. *Arch. Rational Mech. Anal.* 7 (1961) 388–401.
26. C. Pozrikidis, The instability of a moving viscous drop. *J. Fluid Mech.* 210 (1989) 1–21.
27. E. Goursat, *A Course in Mathematical Analysis*. New York: Dover Publications (1964) Vol. II, 389pp.